

CRACK STABILIZATION IN A BRITTLE BODY USING STIFFENERS

A. D. Zaikin

UDC 539.3

The behavior of a crack under uniaxial tension in the presence of reinforcement is studied. The reinforcing members (riveted stiffeners) are modeled by point loads. Only four members nearest to the crack are taken into account. It is shown that stiffeners allow one to arrest a crack and prevent its catastrophic growth. Relations between the geometrical and force characteristics for which the crack is stabilized are obtained. The stabilization mechanism is discussed.

Key words: crack, stress intensity factor, stiffeners, stabilization.

Catastrophic crack growth resulting in failure of a structure can be prevented by using stiffeners (attached riveted members). Morozova and Parton [1] modeled a crack stiffener under uniaxial tension by constant opposite point loads. Only four rivets nearest to the crack were taken into account, and the effect of other rivets was assumed to be negligibly small. Their calculations showed that for certain combinations of geometrical parameters, the crack is stabilized, i.e., a stable transient-equilibrium state occurs. Calculations based on the Barenblatt fracture model were performed under the assumptions of an incompressible material and plane-strain conditions.

Using the Fourier transform and a Cauchy type singular integral equation, Parihar and Latitha [2] obtained the stress intensity factor (SIF) of a crack subjected to four symmetric point loads. Savruk [3] derived an expression for the SIF that, for the particular case of two forces acting on the center lines of the crack, coincides with the solutions obtained by different methods.

The effect of stiffeners on crack behavior was thoroughly studied by Kozeko [4, 5] using a formulation similar to that considered in [1]. The Neuber–Novozhilov integral criterion was used as a fracture criterion. The existence of a stable transient-equilibrium state of the crack was supported by numerous calculations. It is argued [4, 5] that the solution obtained therein differs from the solution of [2, 3], which contains discontinuities of the second kind is therefore questionable. In the present paper, the correctness of the solution of [2] is proved and it is used to study the mechanism of crack stabilization.

We consider an infinite plate weakened by a crack of length $2L$ and subjected to uniaxial tension. The plate is loaded by the stress σ_∞ at infinity. The stiffeners (rivets) are modeled by four point loads N symmetric about the crack axis. The crack configuration, loading conditions, and coordinate axes are shown in Fig. 1.

For uniaxial tension, the mode I SIF is given by

$$K_I^0 = \sqrt{\pi L} \sigma_\infty. \quad (1)$$

For the four point loads modeling the stiffeners, the SIF is given in [2, 3]:

$$K_I^1(b, h) = -2N\sqrt{L/\pi} \operatorname{Re}[(L^2 - z^2)^{-1/2} - 2ihz(L^2 - z^2)^{-3/2}/(\varkappa + 1)]. \quad (2)$$

Here $z = b + ih$, $\varkappa = 3 - 4\nu$ for plane strain (ν is Poisson's ratio) and $\varkappa = (3 - \nu)/(1 + \nu)$ for plane stress.

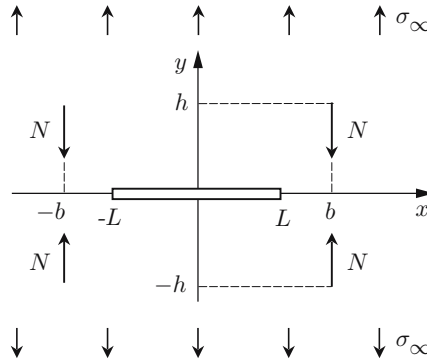


Fig. 1. Orientation of the stiffeners with respect to the crack.

Transforming the expression $L^2 - z^2 = L^2 + h^2 - b^2 - 2ibh = r e^{-i\theta}$, in which

$$r^2 = (L^2 + h^2 - b^2)^2 + (2bh)^2, \quad \tan \theta = 2bh/(L^2 + h^2 - b^2), \quad (3)$$

we obtain

$$(L^2 - z^2)^{-k/2} = r^{-k/2}[\cos(k\theta/2) + i \sin(k\theta/2)], \quad (4)$$

$$2ihz(L^2 - z^2)^{-k/2} = 2hr^{-k/2}\{-h \cos(k\theta/2) - b \sin(k\theta/2) + i[b \cos(k\theta/2) - h \sin(k\theta/2)]\}.$$

Substituting (4) into (2), we obtain a more convenient expression for calculating the mode I SIF:

$$K_I^1(b, h) = -2N \sqrt{\frac{L}{\pi}} \left(\frac{\cos(\theta/2)}{\sqrt{r}} + \frac{2h}{(\varkappa + 1)\sqrt{r^3}} [h \cos(3\theta/2) + b \sin(3\theta/2)] \right). \quad (5)$$

The function $\arctan(y/x)$ is given by

$$\arctan(y/x) = \text{Arctg}(y/x) + m\pi, \quad m = \begin{cases} 1, & x < 0, y > 0, \\ 0, & x \geq 0, \\ -1, & x < 0, y < 0, \end{cases}$$

where $-\pi/2 \leq \text{Arctg}(y/x) \leq \pi/2$ is the principal value of the arc tangent. Therefore, the angle θ in (3) should be calculated taking into account that $m = 1$ for $L^2 + h^2 < b^2$. According to [4, 5], it is in the curve of $L^2 + h^2 = b^2$ where discontinuity of solution (2) occurs.

Figure 2 shows isolines of the dimensionless function $-K_I^1(b, h)\sqrt{L}/N$ that are calculated by (5) for $\varkappa = 2$. The solution has no discontinuities. It is most likely that the discontinuities mentioned in [4, 5] arose from an incorrect calculation of the function $\arctan \theta$. The shape of the isolines shown in Fig. 2 allows one to estimate the effect of the stiffener location on the mode I SIF. It should be noted that according to the problem formulation, the stiffeners cannot be located at the crack tip. Using simple and compact solution (5), one can easily study the behavior of the crack for various parameters of the stiffeners. From (5), it follows that the mode I SIF increases as the axial spacing between the stiffeners decreases and it decreases as the transverse spacing increases.

Since the stress intensity factors (1) and (2) have opposite signs, the combined action of uniaxial tension and the stiffeners can result in a negative value of the total SIF. This problem, corresponding to rather strong stiffeners, arises when the crack faces overlap (this situation is not considered in the present paper).

According to Irwin's fracture criterion, a crack starts to grow when the SIF reaches the critical value K_{Ic} , which is the material constant. In this case, the crack-initiation condition is written as

$$K_I^0 + K_I^1(b, h) \geq K_{Ic}. \quad (6)$$

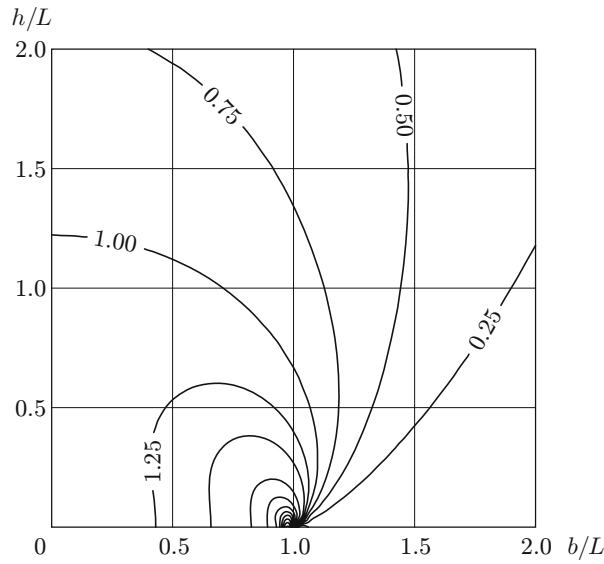


Fig. 2. Isolines of the function $-K_I^1(b, h)\sqrt{L}/N$.

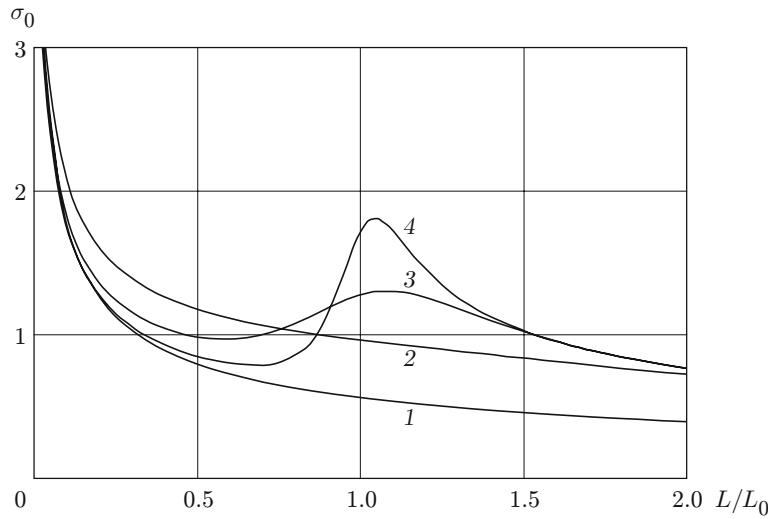


Fig. 3. Crack-initiation stress versus crack length for an unstiffened plate (curve 1) and a stiffened plate at $b = L_0$ and $h = 1.5L_0$ (2), $0.4L_0$ (3), and $0.15L_0$ (4).

Using (1) and (6), we determine the stress that causes a crack of length $2L$ to grow catastrophically:

$$\sigma_\infty(L) \geq (K_{Ic} - K_I^1(b, h))/\sqrt{\pi L}. \quad (7)$$

In addition to the crack length, we determine the characteristic linear dimension of the problem in the form $L_0 = (N/K_{Ic})^2$. Then, in addition to the function $\sigma_\infty(L)$, we construct the dimensionless function $\sigma_0(L/L_0) = \sigma_\infty(L)\sqrt{L_0}/K_{Ic}$.

Figure 3 shows a curve of $\sigma_0(L/L_0)$ for an unstiffened plate (curves 1). This curve (in fact, this is a classical Griffith's curve) implies that when the SIF reaches the critical value K_{Ic} , the crack length increases catastrophically, i.e., the body fails. In the presence of stiffeners, the behavior of the crack changes significantly (curve 2). For certain combinations of the parameters, the crack behavior follows a different scenario (curves 3 and 4 in Fig. 3). The fact that curves 3 and 4 contain segments with a positive derivative of the function $\sigma_0(L/L_0)$ suggests that the crack growth can be stabilized.

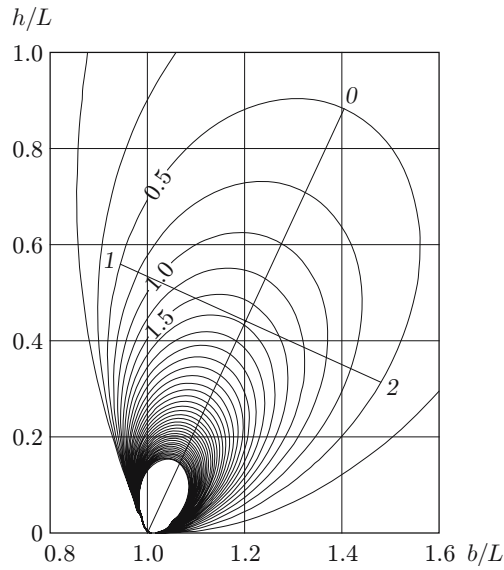


Fig. 4. Isolines of the function $H(b, h)$.

The crack behavior in this regime is described in [1, 4, 5]. When the load reaches the critical value, there is a sudden transition (an increase in the crack length) to another stable state that corresponds to the segment with the positive derivative. A further increase in the load leads to stable crack growth to certain dimensions with subsequent catastrophic failure of the body.

The segment of the Griffith curve that corresponds to stable crack growth is possible if

$$\frac{d\sigma_{\infty}(L)}{dL} \geq 0. \quad (8)$$

In view of (2) and (7), condition (8) becomes

$$H(b, h) \geq H_0, \quad (9)$$

where

$$4H_0 = \sqrt{\frac{\pi L}{L_0}}; \quad H(b, h) = -\frac{L^3}{\sqrt{r^5}} \left(\frac{6h}{\varkappa + 1} [h \cos(5\theta/2) + b \sin(5\theta/2)] + r \cos(3\theta/2) \right).$$

The function $H(b, h)$ depends on the location of stiffeners, and the right side of inequality (9) on the material properties and magnitude of the point loads. Using inequality (9), one can determine the location of the stiffeners that ensures stable crack growth (crack stabilization).

Figure 4 shows isolines of the function $H(b, h)$ for $\varkappa = 2$. The closed lobe-like isolines are inclined at an acute angle to the crack-propagation direction. Given K_{Ic} and N , one can determine an isoline with the following property: the stiffening members corresponding to the points enclosed by this curve ensure crack stabilization. The zero isoline bounds a region outside which stabilization is impossible. One can see from Fig. 4 that for $b = 0$, it is impossible to stabilize the crack using two stiffeners located symmetrically about the crack. Increasing the load N leads to an increase in the region corresponding to the location of the stiffener that ensures crack stabilization.

The shape and position of the isolines $H(b, h)$ and $K_1^1(b, h)$ allow the stabilization mechanism due to the presence of stiffeners to be explained. Let the location of a stiffener be determined by the coordinates (b_s, h_s) . For definiteness, we assume that the axial spacing between the stiffeners (in the direction of the crack) is greater than the crack length: $b_s > L$. Once the initiation condition is satisfied, the crack starts to grow. If, however, the crack length increases, the position of the stiffeners relative to the crack varies. In the process, the spacing between the stiffeners normalized by the crack length decrease in both the direction of the crack axis and in the perpendicular direction. An increase in the crack length may be thought of as a shift of the stiffener along the line $h = bh_s/b_s$ toward the coordinate origin. This shift results in an increase in the mode I SIF due to the presence of stiffeners $K_1^1(b, h)$ (see Fig. 2); the increase being dependent on the initial location of the stiffeners. Despite the

fact that according to (1), K_I^0 also increases, there exist values of (b_s, h_s) for which the total value of the mode I SIF decreases. In this case, the condition for crack initiation is not satisfied and the crack is stabilized.

Let us study the main characteristics of the isolines $H(b, h)$. We first determine the axis of the isoline lobes. We set $z = L(1 + \rho e^{i\varphi})$. Then, for the given ρ_0 , there exists a value of the angle φ_0 for which the function $H(\rho, \varphi)$ reaches a maximum value. The condition $dH(\rho, \varphi)/d\varphi = 0$ uniquely defines the function $\varphi_0(\rho_0, \varkappa)$. An analytical expression for the function $\varphi_0(\rho_0, \varkappa)$ is difficult to obtain, but we can study the behavior of the function $H(\rho, \varphi)$ for $\rho \ll 1$ and $\rho \gg 1$.

For small $\rho \ll 1$, the function $\varphi_0 = \varphi_0(\rho_0, \varkappa)$ can be determined by expanding Eq. (9) into a series. If $\omega = \varphi/2$, keeping the first two terms of the series we obtain

$$H(\rho, \omega) = -\frac{3}{4\sqrt{2}(\varkappa+1)\rho^{3/2}} \left(\sin 7\omega - \frac{2\varkappa+5}{3} \sin 3\omega - \frac{\rho}{4} [\sin 5\omega - (2\varkappa+1) \sin \omega] \right). \quad (10)$$

Equating the derivative of (10) with respect to ω to zero, we obtain

$$28 \cos 7\omega - 4(2\varkappa+5) \cos 3\omega - 5\rho \cos 5\omega + \rho(2\varkappa+1) \cos \omega = 0. \quad (11)$$

For $\varkappa = 1$ and $\rho = 0$, the equation given above has the roots $\omega_1 = \pi n/5$ and $\omega_2 = \pi n$ ($n = 0, 1, \dots$). The root $\omega_1 = \pi/5$ is of interest. For arbitrary \varkappa and ρ , Eq. (11) reduces to a cubic equation for $\cos^2 \omega$. Solving this equation, of the three real roots of this equation, one should choose the root that coincides with the root ω_1 for $\varkappa = 1$ and $\rho = 0$.

The solution can be obtained by a different method. For $\rho < 1$, the exact value of the root of the cubic equation differs from the value of ω_1 by not more than 6° . Therefore, solution (11) can be written as $\omega = \pi/5 - \alpha$, where $\alpha \ll 1$. Substituting this expression for ω into (11) and retaining only terms linear in the small parameter, we obtain α . Passing to the angle φ , we have

$$\varphi_0 = \frac{2\pi}{5} - \frac{2(\varkappa-1)}{3\varkappa+32} \cot\left(\frac{2\pi}{5}\right) - \rho_0 D(\varkappa), \quad (12)$$

where $D(\varkappa) = \sqrt{5(5+2\sqrt{5})/[80(3\varkappa+32)^2](4\varkappa+a_1)(4\varkappa+a_2)}$ and $a_{1,2} = 4 + 10\sqrt{5} \pm \sqrt{2}\sqrt{325\sqrt{5}-663}$.

We now study the behavior of the function $H(b, h)$ far from the crack tip. Bearing in mind that $\rho \gg 1$ in this case, from (9) we obtain

$$H(\rho, \varphi) = -\frac{(\varkappa+4) \sin 3\varphi - 3 \sin 5\varphi}{(\varkappa+1)\rho^3}. \quad (13)$$

Solution of the equation $dH(\rho, \varphi)/d\varphi = 0$ for $\varkappa = 1$ yields $\varphi_0 = \pi/4$. For $1 < \varkappa \leq 3$, an approximate solution can be constructed using the fact that it is close to $\pi/4$. Setting $\varphi_0 = \pi/4 - \alpha$ and bearing in mind that $\alpha \ll 1$, we infer that

$$\varphi_0 = \pi/4 - (\varkappa-1)/(3\varkappa+37). \quad (14)$$

For arbitrary ρ , the equation $dH(\rho, \varphi)/d\varphi = 0$ is solved numerically. Figure 5 shows the calculation results for $\varkappa = 1, 2$, and 3 (curves 1, 2, and 3, respectively). Substitution of ρ_0 and $\varphi_0(\rho_0, \varkappa)$ into (9) yields the value of the isoline $H_{\max} = H(\rho_0, \varphi_0)$. The calculation results for $\varkappa = 2$ are given in Fig. 5 (curve 4). The curves calculated for other values of \varkappa almost coincide with curve 4 for this scale.

Curves 2 and 4 in Fig. 5 are good approximations of the equation $\varphi_0 \approx 71.91 - 8.072\rho_0 + 0.979\rho_0^2 + 4.221 \times 10^{-3}\rho_0^3 - 0.01138\rho_0^4 + 9.154 \cdot 10^{-4}\rho_0^5 - 2.2657 \cdot 10^{-5}\rho_0^6$ (φ_0 is measured in degrees) and $H_{\max} \approx 0.3149\rho_0^{-2.195}$. In addition to the asymptotic expressions constructed, these relations allow one to calculate the parameters of any isoline.

To estimate the transverse dimension of the lobe, we draw two mutually perpendicular axes for the isoline of the function $H(b, h) = \text{const}$. The major axis connects the crack tip to the farthest point on the isoline. The minor axis bisects the major axis. In Fig. 4, these constructions are given for the isoline $H_0 = 0.5$. The points at which the axes intersect the isoline (points 0, 1, and 2) have the coordinates (b_0, h_0) , (b_1, h_1) , and (b_2, h_2) , respectively. In this case, the relations $\varphi_i = \varphi_0 \pm \gamma_i$ and $\rho_0/2 = \rho_i \cos \gamma_i$ are satisfied for $i = 1, 2$. Denoting the minor and major

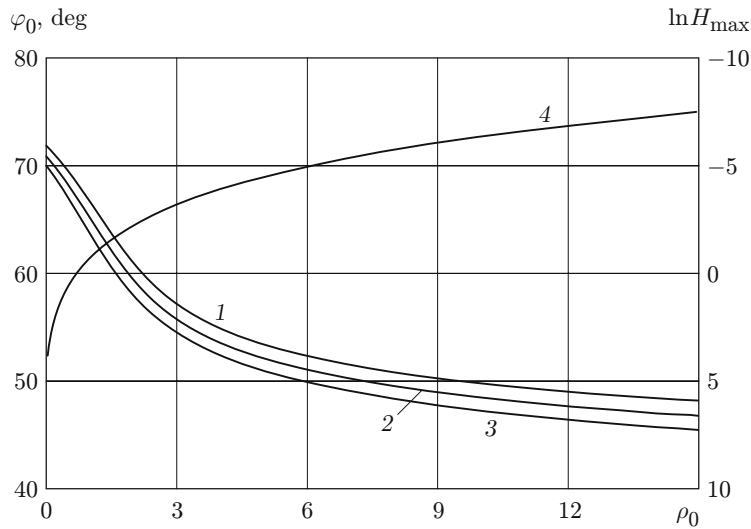


Fig. 5. Slope of the lobe axis of the isoline of the function $H(b, h)$ to the crack (curves 1–3) and the value of the isoline of the function $H(b, h)$ (curve 4) versus the longitudinal dimension of the lobe: $\varkappa = 1$ (1), 2 (2 and 4), and 3 (3).

axes by q and p , respectively, we obtain $q/p = (\tan \gamma_1 + \tan \gamma_2)/2$. The asymptotic equation $H(b_0, h_0) = H(b_i, h_i)$ becomes

$$(2 \cos \gamma_i)^n g(\varphi_0 \pm \gamma_i) = g(\varphi_0). \quad (15)$$

Here $n = 3/2$, $g(\varphi_0) = ((2\varkappa + 5) \sin(3\varphi_0/2) - 3 \sin(7\varphi_0/2))$, where φ_0 is calculated by (12) for $\rho_0 \ll 1$, and $n = 3$ and $g(\varphi_0) = ((\varkappa + 4) \sin(3\varphi_0) - 3 \sin(5\varphi_0))$, where φ_0 is calculated by (14) for $\rho_0 \gg 1$. Equation (15) was solved numerically. For $\varkappa = 1, 2$, and 3, the following values of γ_1 and γ_2 were obtained: $\gamma_1 = 27.92, 29.17$, and 30.17 and $\gamma_2 = 31.44, 33.30$, and 34.70 for $\rho_0 \ll 1$; $\gamma_1 = 19.11, 19.78$ and 20.38 and $\gamma_2 = 27.25, 29.55$, and 31.07 for $\rho_0 \gg 1$.

Thus, the isoline lobe is nearly symmetric. The major axis divides the minor axis into segments which differ by not more than 10%. The ratio of the major axis to the minor axis varies in the range $q/p \approx 0.43-0.63$. The ratio increases as the crack tip is approached and as \varkappa increases.

REFERENCES

1. E. A. Morozova and V. Z. Parton, "On the effect of reinforcement on the crack growth," *Prikl. Mekh. Tekh. Fiz.*, No. 5, 112–114 (1961).
2. K. S. Parihar and S. Latitha, "Griffith cracks in an elastic medium in which body forces are acting," *Eng. Fract. Mech.* **22**, No. 1, 135–148 (1985).
3. M. P. Savruk, "Stress intensity factors in cracked bodies," in: V. V. Panasyuk (ed.), *Fracture Mechanics and Material Strength: Handbook* [in Russian], Vol. 2, Naukova Dumka, Kiev (1988).
4. M. E. Kozeko, "Stress intensity factor in the problem of a crack in the presence of stiffeners," in: *Dynamics of Continuous Media* (collected scientific papers) [in Russian], No. 113, Inst. of Hydrodynamics, Sib. Div., Russian Acad. of Sci., Novosibirsk (1998), pp. 81–85.
5. M. E. Kozeko, "Behavior of a crack in a brittle body in the presence of forces modeling crack arresters," Candidate's Dissertation in Tech. Sci., Novosibirsk (1999).